https://doi.org/10.5194/egusphere-2025-5114
Preprint. Discussion started: 15 January 2026

Hourly-Scale Modeling of Storm Transitions in Southern Brazil with Markov Chains

Camilo Ocampo-Marulanda[1,2]; Jefferson Vieira Santos[1]; Julian David Mera-Franco[2], Alvaro Avila-Diaz[3]; Tiago A. E. Ferreira[1], David Henriques da Matta[4], Antonio Samuel Alves da Silva[1]

1 Graduate Program in Biometrics and Applied Statistics, Department of Statistics and Informatics, Federal Rural University of Pernambuco, Recife, 52171-900, Brazil.
2 Water Resources, Engineering and Soil Research Group (IREHISA), School of Natural Resources and Environmental Engineering, Universidad del Valle, 760032, Cali, Colombia.
3 Earth System Science Program, School of Sciences and Engineering, Universidad del Rosario, Bogotá D.C., Colombia.
4 Federal University of Goiás (UFG), Institute of Mathematics and Statistics (IME), Goiânia, 74001-970, Brazil

Correspondence to: Camilo Ocampo-Marulanda (cmarulanda595@gmail.com)

Abstract. Southern Brazil faces escalating flood risk, yet intraday storm dynamics remain under-characterized. This work presents a season-resolved, intraday Variable Length Markov Chain analysis (VLMC) of storm state transitions, using hourly precipitation from 15 INMET stations from 2007 to 2024. Storms were identified and quantified by depth, duration, and intensity, then classified into Moderate, Strong, and Very Strong states. Peak mean intensities reach 9 to 11 mm h^{-1} in mountainous units, compared with maxima near 7 mm h^{-1} on the coast, where mean intensities are about 3 mm h^{-1}. Storms last roughly 11 to 13 hours in the Southern Plateau and Southern Shield, and 15 to 17 hours in the Central Depression and Coastal Plain, indicating greater lowland persistence. Upward transition probabilities increase in summer, with Moderate to Strong and Strong to Very Strong reaching about 0.20 in orographic areas, while persistence of Very Strong ranges from 0.10 to 0.20 in the Southern Shield. In winter, downward transitions to Moderate exceed 0.90 across most of the domain. Chi-square diagnostics support first-order, season-specific chains with stable transition structure. These intraday, spatially resolved probabilities link geomorphology to storm persistence and provide actionable inputs for early warning, zoning, and climate risk management.

Keywords: storm intensity, VLMC, orographic influence, climate variability.

1 Introduction

Precipitation is one of the most important atmospheric elements in the climatic context, with direct impacts on economic activities, water resources, and the daily lives of the population (Agel et al., 2015). In southern Brazil, especially in the state of Rio Grande do Sul, episodes of heavy rainfall and extreme storms have become increasingly frequent and severe, causing flooding, landslides, and social and economic losses (Guedes et al., 2019; Junges et al., 2019; Minuzzi and Lopez, 2013; Ribeiro-Viana et al., 2009; Valente et al., 2023). The growing occurrence of these extreme events raises concerns about changes in regional climate patterns (Avila-Diaz et al., 2020) and demands detailed analyses of their temporal and probabilistic characteristics.

https://doi.org/10.5194/egusphere-2025-5114
Preprint. Discussion started: 15 January 2026

Previous studies have already demonstrated an increase in the frequency and intensity of extreme events in Rio Grande do Sul (Berlato et al., 2007; Junges et al., 2019; Melo et al., 2015). Valente et al., (2023), when analyzing events from the 20th century, observed that years influenced by the El Niño phenomenon tend to show positive precipitation anomalies, while La Niña years are associated with water deficits. This relationship between oceanic patterns and rainfall behavior was also evidenced by Santos; Barbosa-Diniz, (2014), who demonstrated the influence of oceanic indices on the variability of monthly precipitation in Rio Grande do Sul.

Despite these advances, there are still gaps in understanding precipitation behavior on shorter time scales, such as hourly precipitation, and how these events are temporally organized. The characterization of extreme events using statistical tools such as trend analysis, probability distributions, and Markov Chains allows not only for the description of observed patterns but also for the projection of likely future states based on the temporal dependence of the data (Junges et al., 2019).

Markov chains have been widely used to model rainfall data. The first known application was carried out by (Gabriel and Neumann, 1962) using rainfall records from Israel, and numerous applications have been developed since then. More recently, (Wilks, 2011) consolidated these methods, emphasizing their value for simulating precipitation sequences in atmospheric sciences. Previous studies have used Markov chains to analyze precipitation in Brazil, Back (2017) applied a stochastic Markov chain model to study daily precipitation in the state of Santa Catarina, in southern Brazil, describing geographical patterns of rainfall. Similarly, Jale et al., (2019) examined rainfall on a daily scale in three states (dry, humid, and rainy) for the state of Paraíba, in northeastern Brazil. In their study, they reported transition probabilities between states, equilibrium probabilities, and expected durations for the different states. More recently, Vargas; Corso; Vallejos, (2022) applied Markov chains to assess how normal climate patterns may shift to altered states in the future for the city of Caxias do Sul, in the state of Rio Grande do Sul. They used the results of Markov modeling to support agricultural planning in the context of climate change.

The present study proposes an integrated analysis of the temporal and probabilistic behavior of storms in southern Brazil, with an emphasis on the eastern portion of the Rio Grande do Sul state, consists of the Jacuí Basin, the São Gonçalo Basin, and rivers that flow directly into the Atlantic Ocean - Drainage Area of the Lagoons (DAL), using hourly precipitation data from the Instituto Nacional de Meteorologia (INMET). The study aims to characterize storms and model the transitions through Markov chains.

Recent hydrometeorological disasters in southern Brazil, including the September 2023 crisis and the unprecedented rainfall of April to May 2024, expose systemic vulnerabilities in flood preparedness and motivate analyses that resolve storm evolution at intraday scales (Alvalá et al., 2024; Collischonn et al., 2025). Most regional climatologies emphasize annual signals (Berlato et al., 2007; Guedes et al., 2019; Junges et al., 2019; Minuzzi and Lopez, 2013), monthly or seasonal behavior (Britto et al., 2006; Marques and Möller, 2008; Santos and Barbosa Diniz, 2014; Valente et al., 2023), or daily statistics (Dorneles et al., 2020; Melo et al., 2015; Sanches et al., 2019; Schumacher et al., 2016; Teixeira and Prieto, 2020a), leaving intraday persistence and transition dynamics underexplored. Addressing this gap, we use hourly precipitation from 15 stations from 2007 to 2024 to identify storms, quantify depth, duration, and intensity across contrasting physiographic units, and

https://doi.org/10.5194/egusphere-2025-5114
Preprint. Discussion started: 15 January 2026

estimate season-specific transition probabilities among intensity states with Variable Length Markov Chains. This intraday, state-based framework yields spatially and seasonally resolved metrics of intensification and persistence that can feed early warning, strengthen risk mapping, and support the revision of hydrologic design criteria in flood-prone basins. The structure of the document is organized as follows. Chapter 2 presents a description of the study area and the precipitation data used. Chapter 3 details the methodology applied for storm characterization and Markov chain modeling. Chapter 4, presents and maps the results, followed by a discussion in light of the existing literature. Finally, Chapter 5 provides the main conclusions of the study.

2 Study area and precipitation data

The study area is located in southern Brazil, in the state of Rio Grande do Sul (see Figure 1a). The eastern portion consists of the Jacuí Basin, the São Gonçalo Basin, and rivers that flow directly into the Atlantic Ocean (see Figure 1b). Collectively, we refer to this as the Drainage Area of the Lagoons (DAL). In this region, rivers drain into the large lagoons of southern Brazil, including Lagoa dos Patos, Lagoa Merín, and Lagoa Mangueira (Marques; Möller, 2008).

The Jacuí Basin discharges its waters into Lagoa dos Patos via the Guaíba River, on which the city of Porto Alegre is located (see Porto Alegre station in Figure 1), the main city in southern Brazil. The São Gonçalo Basin, in turn, acts as a natural channel connecting Lagoa dos Patos and Lagoa Mirim, regulating water flow in the lower part of the system (Marques; Möller, 2008).

A total of 15 weather stations with hourly data from 2007 to 2024 were used. These data are publicly available from the Instituto Nacional de Meteorologia (INMET) at https://portal.inmet.gov.br/dadoshistoricos. The spatial distribution of the stations is evenly spread across DAL, as shown in Figure 1c, and the statistical basic data of the stations are presented in Table 1.

The mountainous region of DAL is concentrated in the north, in the Souther Plateu, reaching a maximum elevation of 1,373 meters above sea level (m a.s.l.) (See Figure 1). In the south, the terrain features slightly lower mountains, around 300 m a.s.l., in the Souther Shield. Meanwhile, the lowland areas are prone to prolonged flooding, particularly in the Central Depression and Coastal Plain (Valente et al., 2023).

https://doi.org/10.5194/egusphere-2025-5114
Preprint. Discussion started: 15 January 2026

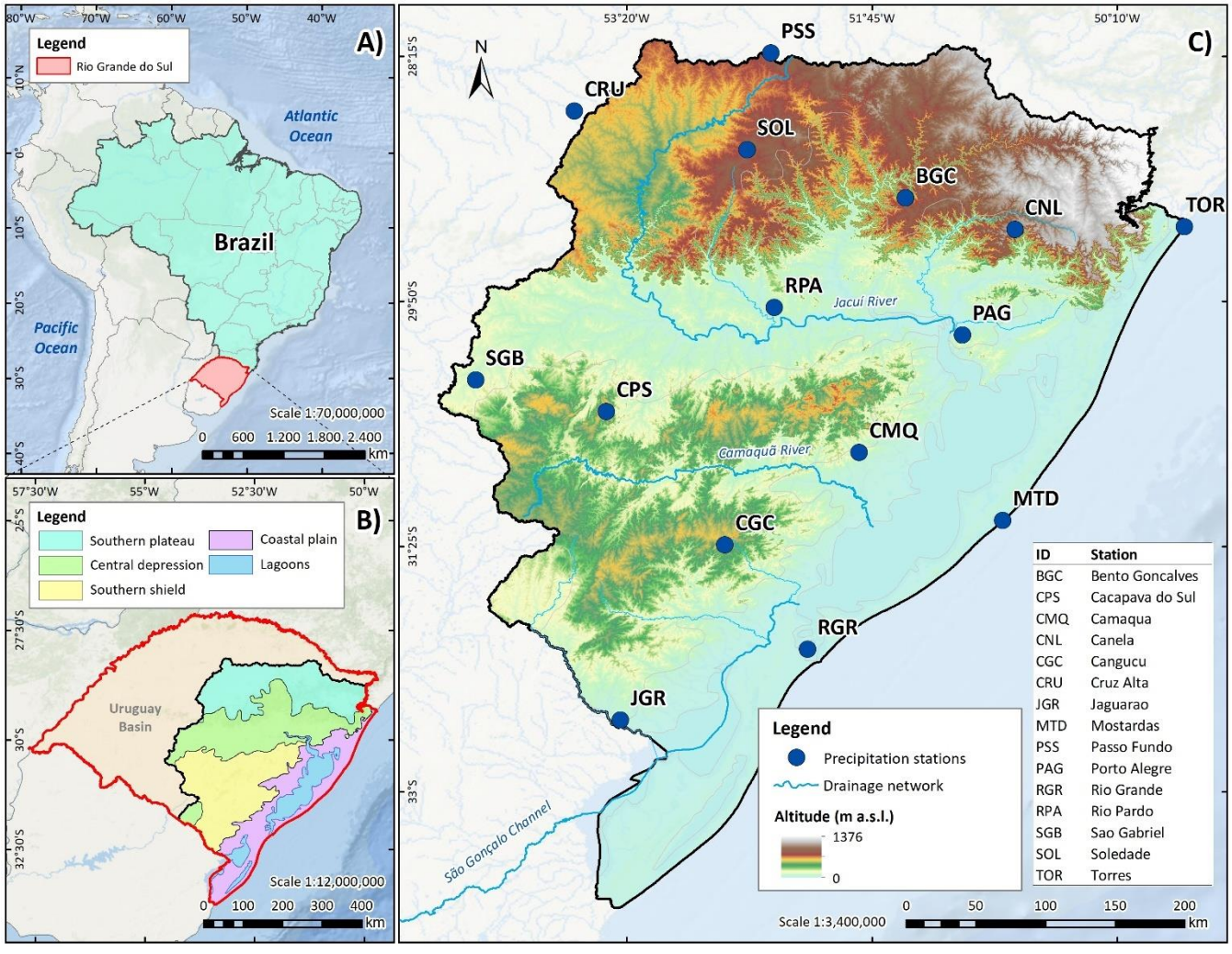

Figure 1. Localization of the Drainage Area of the Lagoons (DAL) and weather stations

Table 1. Basic statistical description of the rainfall stations with hourly data used

Station	ID	Mean (mm)	Maximum precipitation (mm)	Desvest (mm)	Missing data (%)
Bento Goncalves	A840	0.19	56.8	1.19	3.46
Cacapava do Sul	A812	0.2	45.8	1.26	3.05
Camaqua	A838	0.18	51.4	1.08	5.66
Canela	A879	0.25	59.4	1.22	15.29
Cangucu	A811	0.18	46.4	1.1	8.98
Cruz Alta	A853	0.2	47	1.32	5.04

https://doi.org/10.5194/egusphere-2025-5114
Preprint. Discussion started: 15 January 2026

Jaguarao	A836	0.16	48.8	1.09	6.75
Mostardas	A878	0.13	30.4	0.91	19.62
Passo Fundo	A839	0.21	47.8	1.27	1.23
Porto Alegre	A801	0.18	37.8	1.12	0.75
Rio Grande	A802	0.14	85.8	1.09	7.97
Rio Pardo	A813	0.19	46.4	1.18	4.88
São Gabriel	A832	0.17	76.8	1.21	11.24
Soledade	A837	0.21	47.4	1.33	10.85
Torres	A808	0.18	50	1.09	10.29

3 Methodology

The study utilized 15 hourly precipitation stations provided by INMET. Storm characterization was conducted using the hourly precipitation data as recommended by (Lamjiri et al., 2017). From the characterization of storms, the following variables were obtained: total storm precipitation, storm duration, maximum storm intensity, and average storm intensity.

The maximum storm precipitation data, which is a categorical variable, was taken and the 95th and 99th percentiles were estimated to define the states: Moderate, Strong and Very Strong Storms. These were the states used for Markov chain modeling.

For each station, four season-specific Markov chains were fitted to account for seasonal differences in storm-intensity transitions. Before modeling, the order of the chains was verified with a chi-square test and the homogeneity of the time series. The general scheme of the methodology can be seen in Figure 2.

https://doi.org/10.5194/egusphere-2025-5114
Preprint. Discussion started: 15 January 2026

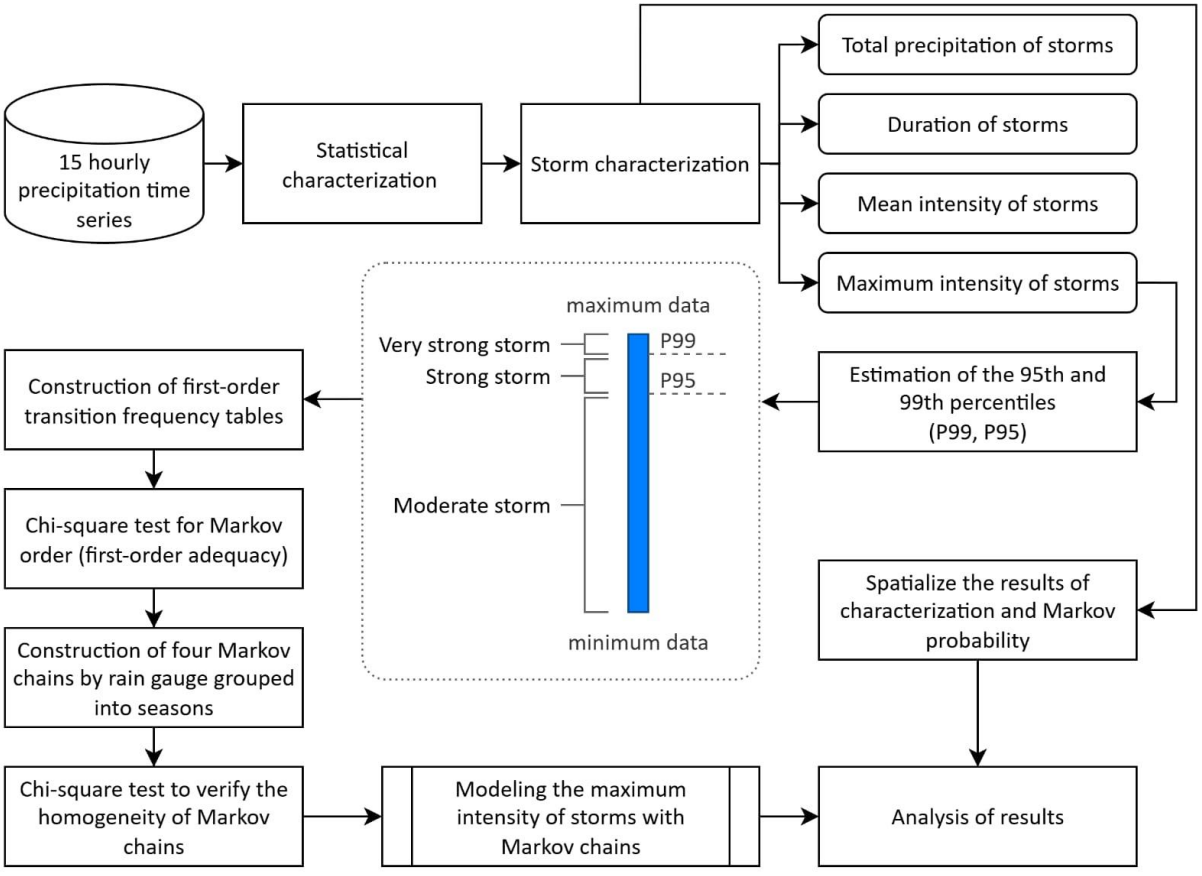

Figure 2. General methodology for storm analysis at hourly scale

105

3.1 Characterization of storms

In this study, hourly precipitation data were used to identify "storms". A storm is defined as a continuous stretch of precipitation separated by at least 6 hours of zero precipitation, with a minimum total precipitation of 5 mm. This criterion for defining a storm was adopted from previous studies to ensure comparability (Lamjiri et al., 2017; Palecki et al., 2005). For each storm,
110 the total precipitation (mm) was estimated as the sum of hourly precipitation values from the start to the end of the event. The storm duration (h) was defined as the number of hours with precipitation greater than 5 mm, from the beginning to the end of the event. The average storm intensity (mm h^{-1}) is the total precipitation divided by the storm duration. Finally, the maximum storm intensity (mm h^{-1}) is the highest hourly precipitation rate observed from the beginning to the end of the event (see Figure 3). The variables characterizing the storm, as defined above, were spatialized as an average over the study basin.

https://doi.org/10.5194/egusphere-2025-5114
Preprint. Discussion started: 15 January 2026

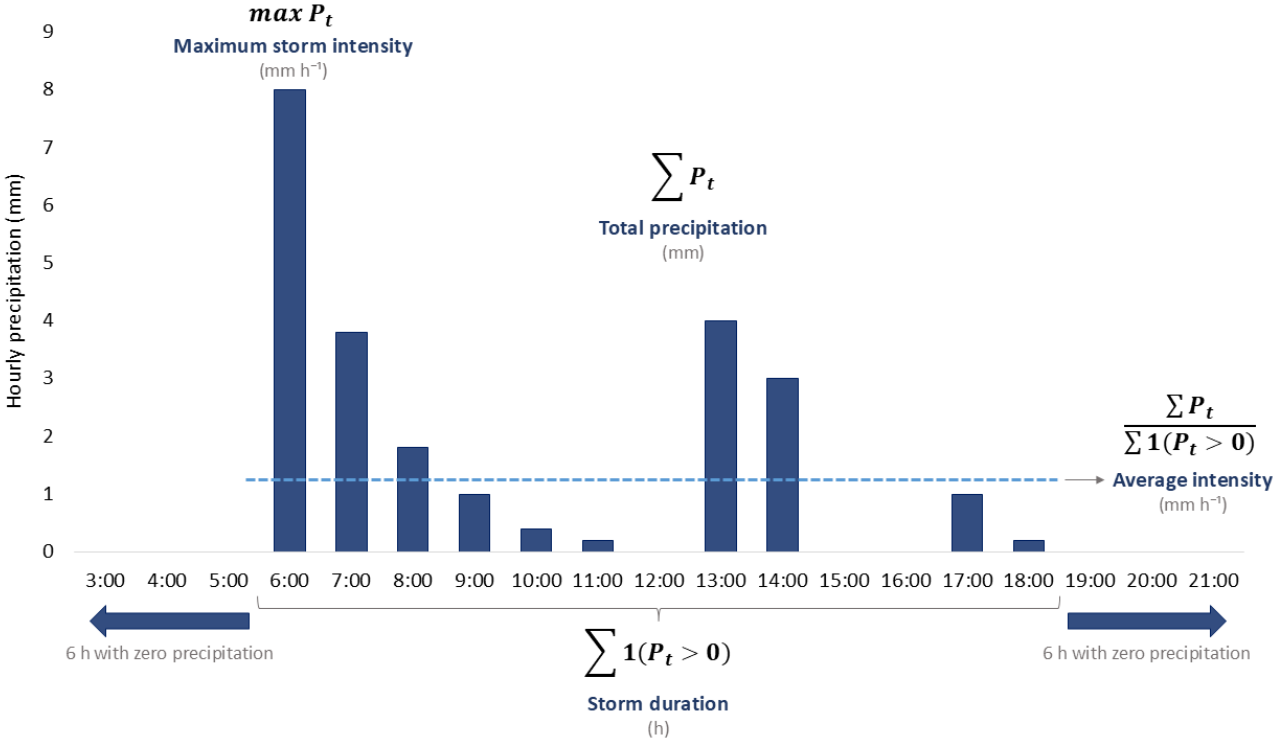

Figure 3. Graphical definition of storm-event metrics and detection criteria

3.2 Methodology for Calculating the Transition Probability Between Storm States using Markov Chains

3.2.1 Organization and discretization of storm intensity data

The variables resulting from the characterization of storms were examined statistically and graphically. An exploratory analysis was performed on the mean, median, standard deviation, and coefficient of variation (Table 1). Stations were grouped according to these variables, frequency histograms and box plots were generated for them, and the data were subsequently analyzed by season.

The seasons of the year were defined based on the dates of the solstices and equinoxes for the southern hemisphere. Summer was defined as December 21 to March 20 (of the following year), fall as March 20 to June 20, winter as June 20 to September 22, and spring as September 22 to December 21.

Considering the statistical analysis, the maximum storm intensity series at each rainfall station were modeled using Markov chains, grouped by season. The 95th and 99th percentiles of the intensity distribution were used as thresholds to define the state boundaries, as shown in Table 2, following approaches adopted by other authors (Gao et al., 2021; Jiang et al., 2023; Kemsley et al., 2024).

Table 2. Classification of rainfall intensity states

https://doi.org/10.5194/egusphere-2025-5114
Preprint. Discussion started: 15 January 2026

States	Criterion
Moderate Storm	Intensity < 18 mm h^{-1}
Strong Storm	Intensity ≥ 18 mm h^{-1} and ≤ 23 mm h^{-1}
Very Strong Storm	Intensity > 23 mm h^{-1}

3.2.2 Evaluation of assumptions for Markovian modeling

First-order dependency was evaluated by comparing observed and expected frequencies in the transition matrices. For each combination of station and season, first-order transition matrices were constructed, representing the probabilities of transitioning from one discrete rainfall intensity state to another in consecutive events. These matrices quantify the conditional probabilities (Eq. 1).

$$P(X_t = j | X_{t-1} = i) \quad (1)$$

where X_t denotes the discrete state of rainfall intensity at time t, and i, j are the possible states (Moderate, Strong, Very Strong).

This formulation embodies the Markovian dependence property (Norris, 1997; Ross, 2014), where the probability distribution of the current state depends only on the immediately preceding state (Eq. 2).

$$P(X_t | X_{t-1},\ X_{t-2}, \dots, X_1) = P(X_t | X_{t-1}) \quad (2)$$

This assumption allows modeling the temporal dynamics through a single-step transition matrix, simplifying estimation and interpretation.

The transition matrix P was constructed by computing the relative frequencies of state transitions over consecutive events, as shown in Eq. (3).

$$P = \begin{bmatrix} P_{11} & P_{12} & P_{13} \\ P_{21} & P_{22} & P_{23} \\ P_{31} & P_{32} & P_{33} \end{bmatrix} \quad (3)$$

Where each element P_{ij} represents the probability of transitioning from state i to state j. The assumption of a first-order Markov process implies that the future state depends only on the present state, simplifying the modeling of storm persistence and progression.

To investigate potential seasonal differences in transition behavior at each station, a chi-square test was applied to the corresponding transition matrices. Rather than treating the data as a single continuous series, the time series at each location

https://doi.org/10.5194/egusphere-2025-5114
Preprint. Discussion started: 15 January 2026

was segmented into four separate Markov chains—one for each of the four seasons: summer, fall, winter, and spring. This approach made it possible to observe seasonal patterns more clearly and assess whether state transition probabilities remained stable within each period. Verifying this internal consistency was key, as it supported the decision to represent each season with a distinct transition matrix, thereby preserving the integrity of intra-seasonal dynamics while avoiding the distortion that could arise from mixing data across different times of the year. The chi-square test was applied to verify the temporal homogeneity of transition probabilities within each season, ensuring that the Markov chain assumptions of stationarity and first-order dependence were satisfied.

3.2.3 Estimation and Application of the Markov Model

The transition probability matrices were estimated by calculating the relative frequencies of transitions between discrete states. These matrices were used to quantify the conditional probability of observing a given rainfall intensity state, given the state of the preceding event (Gabriel and Neumann, 1962; Wilks, 2011). This approach allows simulating future sequences of rainfall intensity by sequential sampling from the estimated transition probabilities (Eq. 4).

$$P(X_t = j | X_{t-1} = i) = \frac{N(i \to j)}{\sum_k N(i \to k)} \quad (4)$$

Where $N(i \to j)$ is the number of transitions observed from state i to j, and the denominator $\sum_k N(i \to k)$ is the total number of transitions departing from i across all possible states k, ensuring that each row of the matrix sums to one. This formulation ensures that the probabilities in each row of the transition matrix sum to one, forming a stochastic matrix. The model provides a framework to assess the likelihood of occurrence of *Moderate, Strong, or Very Strong* events conditioned on antecedent conditions, supporting the analysis of temporal persistence patterns. It is important to note that the Markov assumption implies that the process is memoryless beyond one lag and that the estimated probabilities are assumed constant across the observed period.

To avoid linking events separated by long gaps, each seasonal series (summer, fall, winter, spring) was split by year, and transitions were computed only within the same seasonal block. Here s denotes the season and y the year of observation. At the start of each new season, the chain was "reset," meaning that the first event of the season s in year y is treated as independent of the last event of season s in year $y-1$ (Eq. 5).

$$P\left(X_1^{(s,y)} = j \middle| X_{last}^{(s,y-1)} = i\right) = P(X_1^{(s,y)} = j) \quad (5)$$

This simple reset procedure, inspired by the idea of Variable Length Markov Chains (VLMC) (Bühlmann and Wyner, 1999), prevents spurious transitions between years and yields a more realistic picture of how storms evolve within each season.

4. Results and discussion

4.1 Storm Characterization

The results of the storm characterization are presented in Figure 4. The highest precipitation amounts occur in the Southern Plateau, with average magnitudes of approximately 29 mm per event. Total precipitation shows a decrease, being greater in

https://doi.org/10.5194/egusphere-2025-5114
Preprint. Discussion started: 15 January 2026

the Southern Plateau (north) and decreasing toward the Coastal Plain (south), with a slight increase observed in the mountainous region of the Southern Shield.

The average storm duration is shorter in the mountainous areas of the Southern Plateau and Southern Shield, ranging between 11 and 13 hours, whereas the longest-lasting storms occur in the ocean-facing foothills of the Central Depression and Coastal Plain, ranging between 14 and 17 hours.

Rainfall intensities are higher in the western part of the DAL and lower near the ocean. Consequently, maximum intensities are also greater in the west, particularly in the mountainous zones of the Southern Plateau and Southern Shield, where average peak values range from 9 to 10 mm h^{-1}. In contrast, precipitation intensities are lower in the Coastal Plain, with mean values of 3 mm h^{-1} and maximum intensities averaging around 8 mm h^{-1}.

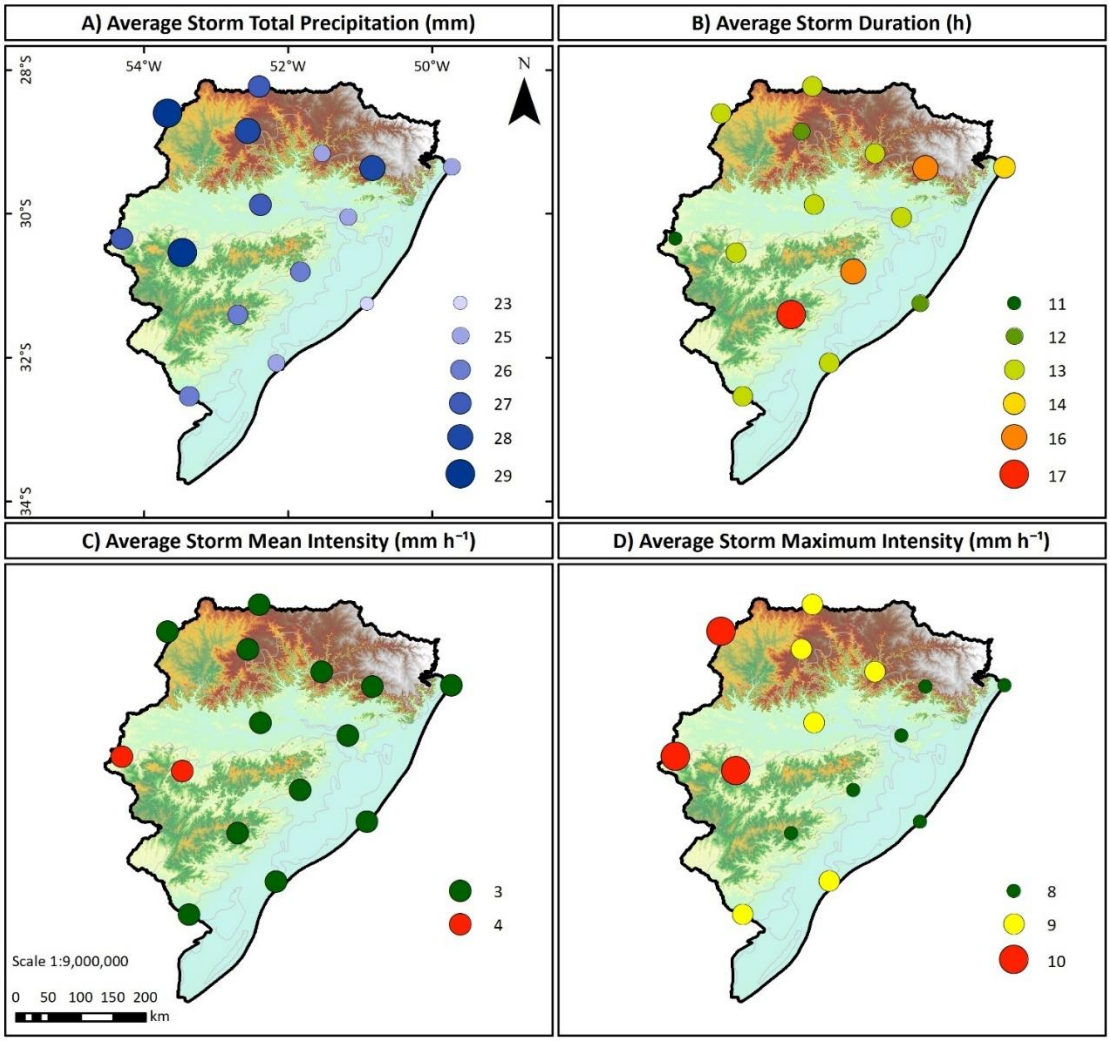

Figure 4. Spatialization of the average storm behavior in terms of (a) magnitude, (b) duration, (c) average intensity and (d) maximum intensity of storms

https://doi.org/10.5194/egusphere-2025-5114
Preprint. Discussion started: 15 January 2026

4.2 Verification of Markov Chain Assumptions and Seasonal Rainfall Intensity Analysis

The time series modeled with Markov chains corresponds to the Average Maximum Rainfall Intensity of the storms characterized in the previous analysis. An exploratory graphical analysis was conducted to evaluate potential seasonal differences. Figure 5 presents boxplots of the data grouped by season.

The results highlight clear seasonal contrasts. During summer, rainfall intensities are higher in terms of magnitude (greater extreme values between 27 mm h^{-1} and 90 mm h^{-1}), frequency (123 outliers), and variability (interquartile range between 5 mm h^{-1} to 14 mm h^{-1}). In contrast, winter exhibits the lowest intensities (extreme values between 18 mm h^{-1} and 48 mm h^{-1}), with fewer extreme events (63 outliers) and reduced variability (interquartile range between 4 mm h^{-1} to 8 mm h^{-1}) compared to the other seasons. Spring and fall display intermediate behavior between the two opposite phases, with spring showing slightly higher rainfall intensities relative to fall.

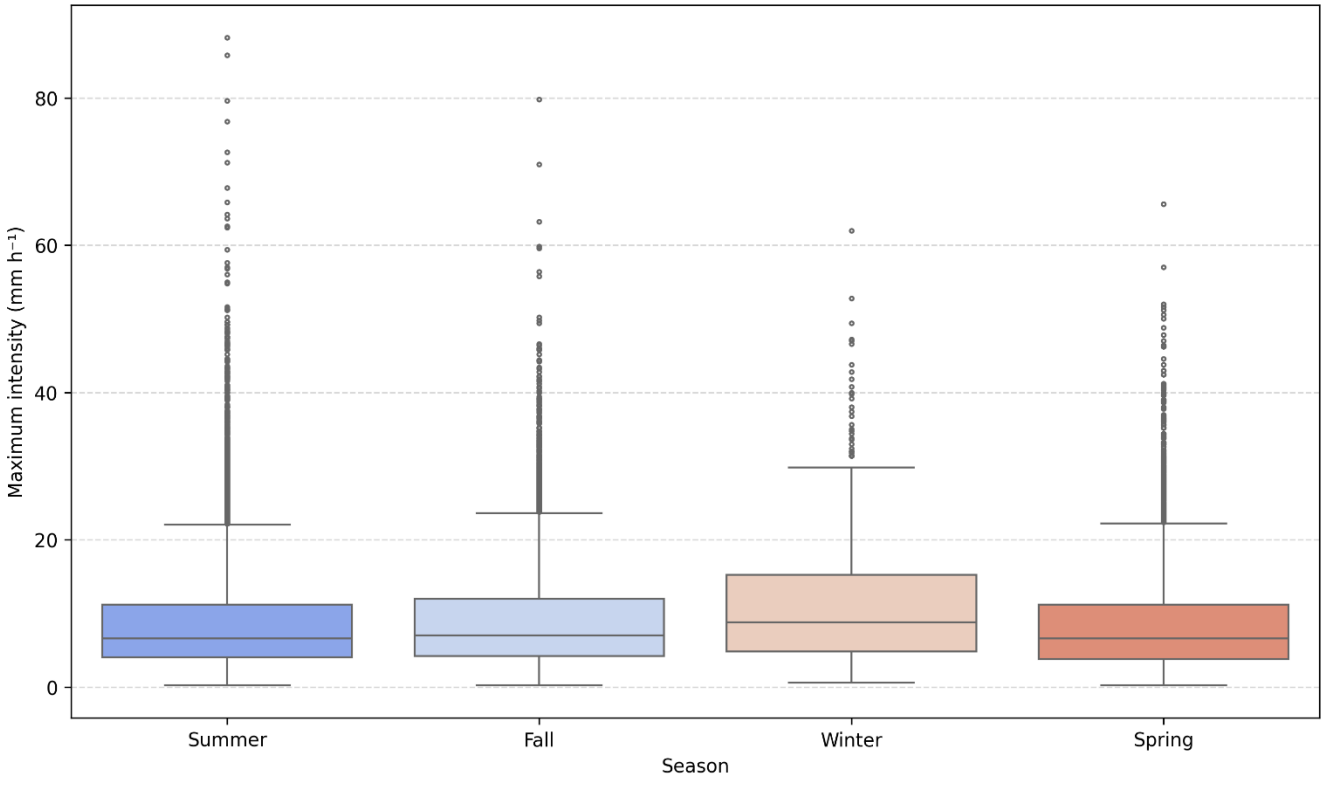

Figure 5. Boxplots of the average maximum rainfall intensity grouped for summer, fall, winter, and spring

Considering the seasonal differences highlighted in Figure 5, four separate time series were constructed, one for each season at every station. First-order transition matrices were then derived, and the order of each chain was verified. The chi-square values and corresponding p-values of this test are presented in Appendix A1. Additionally, the temporal homogeneity of the

https://doi.org/10.5194/egusphere-2025-5114
Preprint. Discussion started: 15 January 2026

Markov chains defined by season was assessed through the transition matrices, with the chi-square statistics and p-values also reported in Appendix A1.

The results indicate that, for each station and season analyzed, the transition matrices exhibit homogeneous behavior consistent with first-order Markov chains. The chi-square statistics and their corresponding p-values were generally not significant ($p > 0.05$), suggesting that transition probabilities do not vary substantially within each station and can be considered stable over time. This outcome reinforces the suitability of applying Markov chains—considering the reset of the VLMC—and validates the results obtained from modeling extreme rainfall events using this approach.

4.3 Spatial Results of Markov Chain Modeling

In this chapter, the transition probabilities between rainfall intensity states are presented, grouped by season: spring (Figure 6), summer (Figure 7), winter (Figure 8), and fall (Figure 9). The interpretation of the transition maps follows this logic: the initial state corresponds to the rows, and the subsequent state to the columns. Therefore, Figures 6b, 7b, 8b, and 9b illustrate the probability of transitioning from the Moderate state (row) to the Strong state (column). The same logic applies to all other cells and figures presented in this chapter.

Figure 6 shows the transition probabilities between rainfall intensity states derived from the Markov chain modeling for spring. Upward transition probabilities, like Moderate to Strong (Figure 6b), Strong to Very Strong (Figure 6f), Moderate to Very Strong (Figure 6c) are relatively low, remaining below 0.2 across the entire study area. In contrast, there is a high probability of downward transitions to the Moderate state, like Strong to Moderate (Figure 6d) and Very Strong to Moderate (Figure 6g), with values exceeding 0.7 throughout the region and particularly pronounced in the Coastal Plain.

Probabilities of transitioning to or persisting in the Strong state remain below 0.1 (Figures 6b, 6e, 6h), although slightly higher in the mountainous regions of the Southern Plateau and Southern Shield. In the lowland areas of the Central Depression and Coastal Plain, the probability of maintaining Strong conditions is nearly zero. The greater persistence of the Strong state in mountainous zones may be attributed to the role of topography in modulating orographic convection, which in spring has not yet reached its peak development.

https://doi.org/10.5194/egusphere-2025-5114
Preprint. Discussion started: 15 January 2026

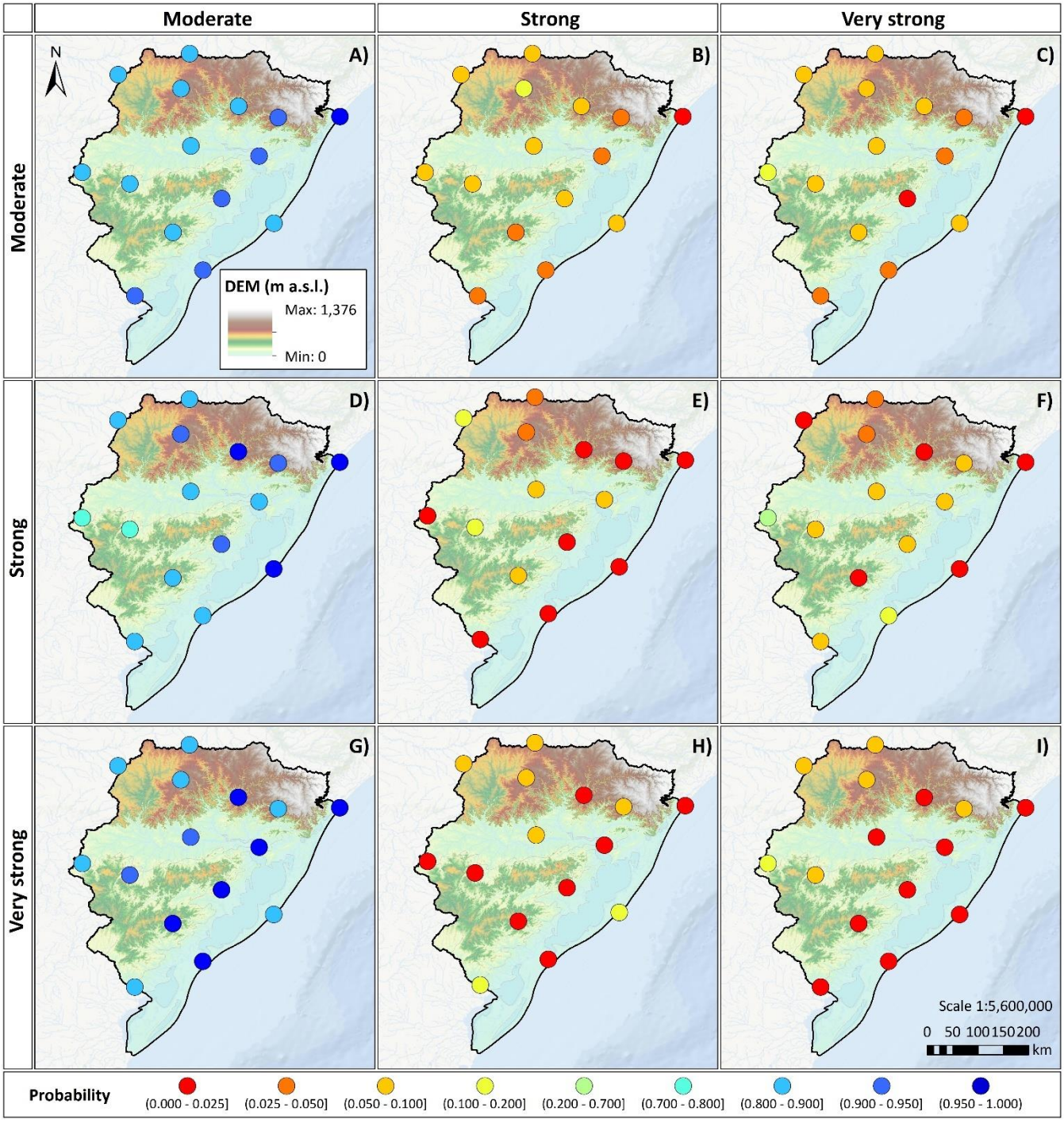

Figure 6. Spatial distribution of Markov transition probabilities between rainfall intensity states during spring

https://doi.org/10.5194/egusphere-2025-5114
Preprint. Discussion started: 15 January 2026

Figure 7 shows the transition probabilities between rainfall intensity states for summer. The probability of maintaining a Moderate storm state ranges between 0.7 and 0.95 (Figures 7a, 7d, 7g), indicating strong persistence. In contrast, the probability of remaining in the Strong or Very Strong states is below 0.2 (Figures 7b, 7c, 7e, 7f, 7h, 7i).

Upward transitions, like Moderate to Strong (Figure 7b), Strong to Very Strong (Figure 7f), and Moderate to Very Strong (Figure 7c) display higher probabilities in summer compared to the other seasons. The probability of a Moderate to Strong transition reaches up to 0.2 in the Southern Shield, while the probability of Strong to Very Strong transitions ranges from 0.025 to 0.2 across the Central Depression and Coastal Plain. Persistence of the Very Strong state can reach 0.2, particularly in the mountainous Southern Shield (Figures 7c, 7f, 7i).

The higher rainfall intensities in the mountainous regions coincide with the peak of convection in the area, where orographic effects enhance air uplift and favor more intense storms. Conversely, in the flat areas of the Central Depression and Coastal Plain, Very Strong events dissipate more quickly. This pattern reflects the typical behavior of plains, where the absence of topographic barriers reduces the persistence of convective systems.

https://doi.org/10.5194/egusphere-2025-5114
Preprint. Discussion started: 15 January 2026

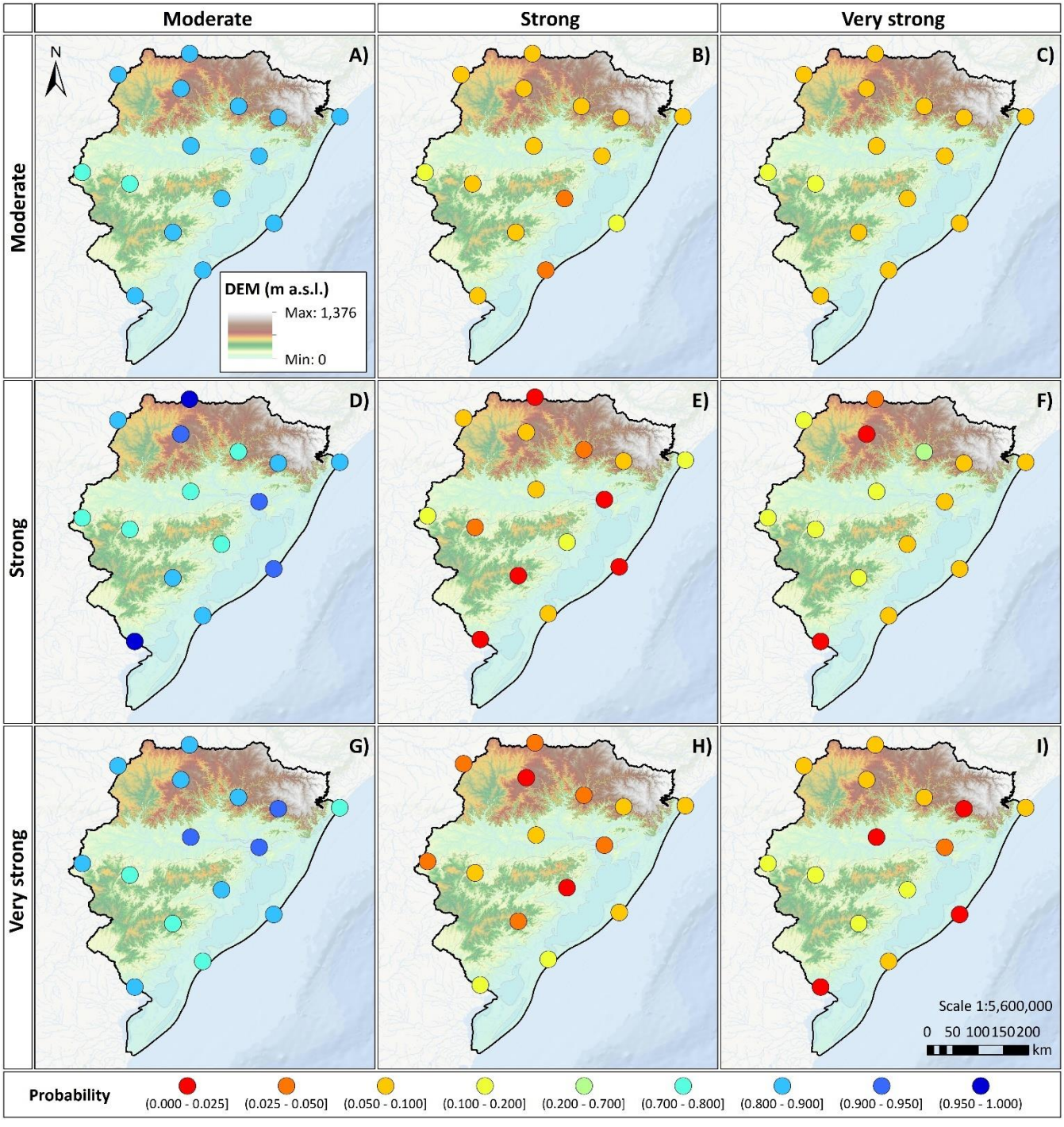

Figure 7. Spatial distribution of Markov transition probabilities between rainfall intensity states during summer

https://doi.org/10.5194/egusphere-2025-5114
Preprint. Discussion started: 15 January 2026

Figure 8 shows the transition probabilities between rainfall intensity states for winter. During this season, extreme events are less frequent, with downward transition probabilities reaching values close to 0.9 (Figures 8a, 8d, 8g). While Upward transition probabilities, like Moderate to Strong (Figure 8b), Strong to Very Strong (Figure 8f), Moderate to Very Strong (Figure 8c) remain near 0.025. The probability of transitioning from Strong to Very Strong (Figure 8f), or of persisting in the Very Strong (Figures 8c, 8f, 8i), is below 0.025 across the entire study area.

In contrast, downward transitions (Strong to Moderate, Very Strong to Moderate) are dominant, with probabilities exceeding 0.9 in most of the region. Unlike summer and spring, winter does not exhibit distinct spatial patterns in the behavior of extreme events, indicating a more homogeneous distribution of rainfall intensity across the study area.

https://doi.org/10.5194/egusphere-2025-5114
Preprint. Discussion started: 15 January 2026

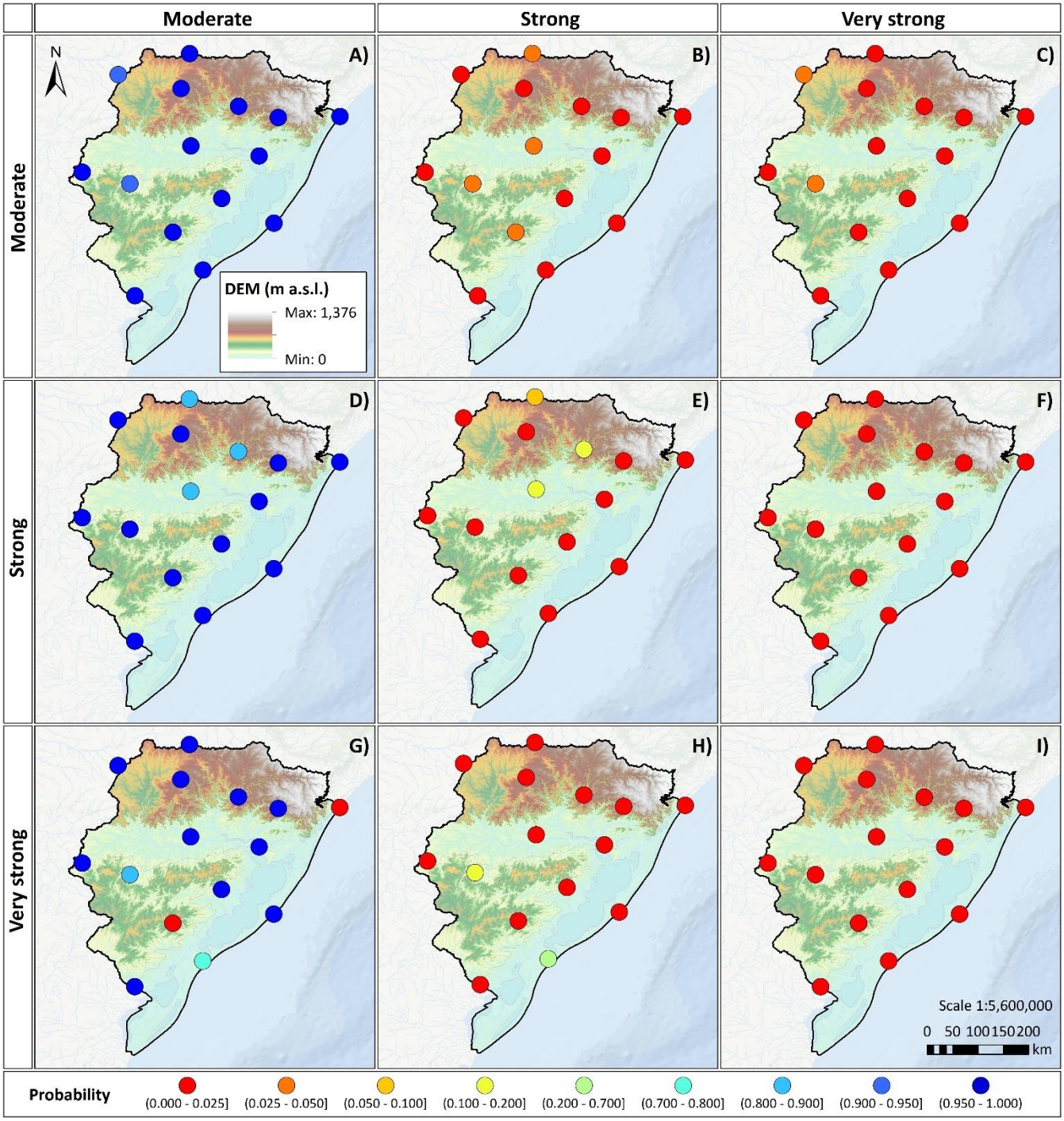

Figure 8. Spatial distribution of Markov transition probabilities between rainfall intensity states during winter

https://doi.org/10.5194/egusphere-2025-5114
Preprint. Discussion started: 15 January 2026

Figure 9 shows the transition probabilities between rainfall intensity states for fall. Upward transition probabilities, like Moderate to Strong (Figure 9b), Moderate to Very Strong (Figure 9c) remain below 0.1 across the study area. Similarly, transitions between the Strong and Very Strong states (Figures 9f, 9h) are generally below 0.2, with slightly higher values observed for the Strong to Very Strong transition (Figure 9f).

https://doi.org/10.5194/egusphere-2025-5114
Preprint. Discussion started: 15 January 2026

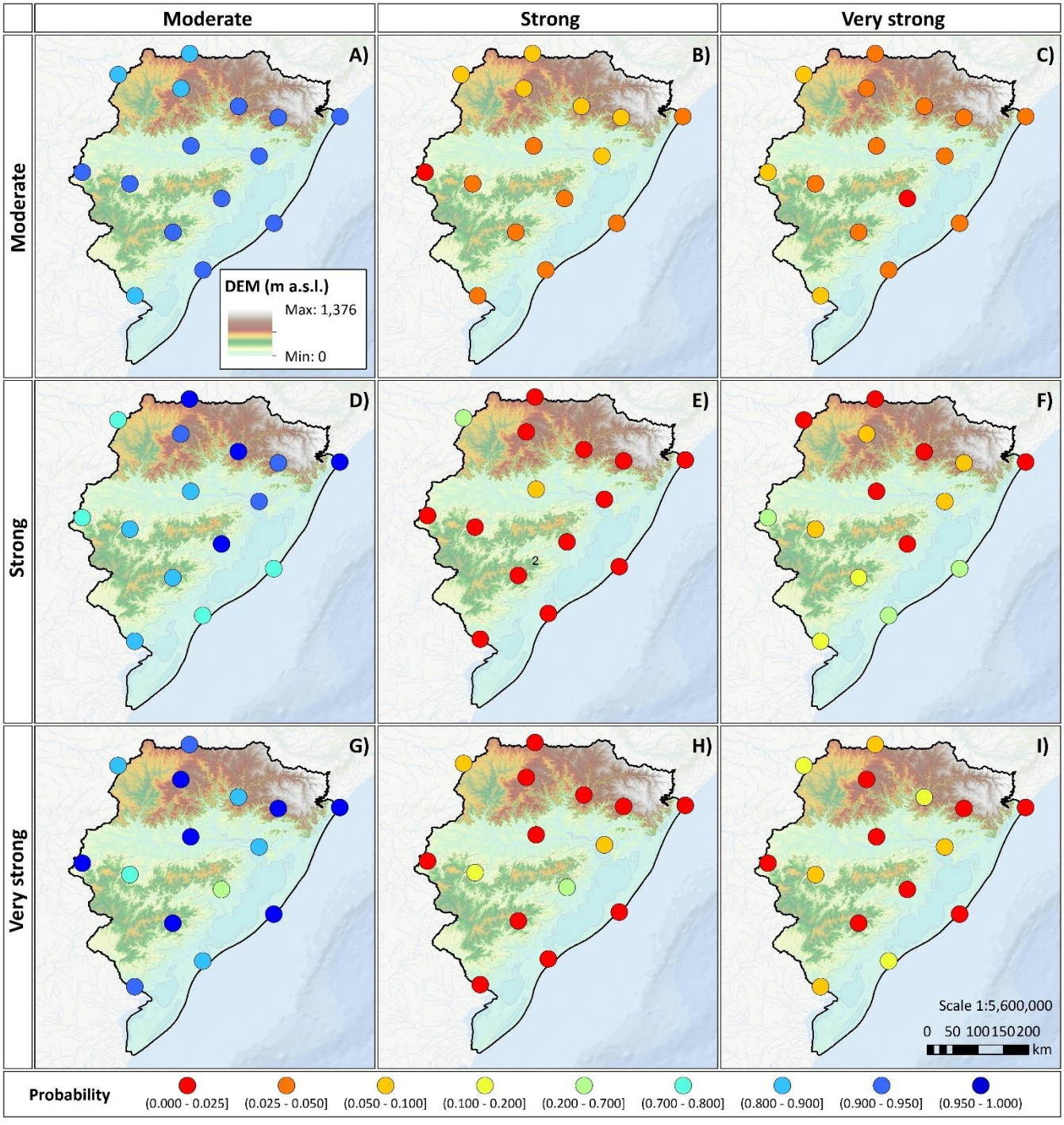

Figure 9. Spatial distribution of Markov transition probabilities between rainfall intensity states during fall

https://doi.org/10.5194/egusphere-2025-5114
Preprint. Discussion started: 15 January 2026

The comparative analysis of rainfall regimes throughout the year reveals well-defined patterns of persistence and transition in storm events, closely linked both to seasonal dynamics and to the particularities of regional topography. In spring, there is a marked tendency for rapid returns to moderate conditions after high-intensity episodes, a phenomenon especially evident in the Coastal Plain. By contrast, in the elevated areas of the Southern Plateau and Southern Shield, the Strong state persists more frequently, suggesting a significant influence of topography in modulating orographic convection.

During summer, rainfall dynamics become more complex: upward transitions to more intense states—Moderate to Strong and Strong to Very Strong—are more frequent, particularly concentrated in the Southern Shield, where topographic conditions act as catalysts of repeated and intense convective processes. In the lowland regions, such as the Central Depression and Coastal Plain, Very Strong events tend to dissipate more quickly, consistent with the absence of orographic forcing mechanisms that sustain convective activity.

Fall, in turn, is characterized by a remarkable stability in rainfall regimes: Moderate events predominate with little variability, and transition probabilities between states remain considerably low. This regularity suggests a more predictable rainfall pattern, marked by a more uniform distribution of precipitation. In winter, by contrast, the highest downward transition rates are observed—exceeding 90%—and sequences of extreme events are rare. This pattern is consistent with the predominance of frontal systems, which tend to generate less intense, more homogeneous, and shorter-lived rainfall.

Taken together, the findings highlight the decisive role of topography in enhancing the intensity and persistence of summer rainfall, as well as the concentration of prolonged flood risk in the lowland areas during winter. These seasonal and spatial differences are of strategic importance for hydrological modeling and for the design of risk management policies tailored to the specific characteristics of the territory.

4.4 Discussing of the results

Our findings indicate higher probabilities of upward transitions (e.g., Strong to Very Strong) during summer, consistent with synoptic studies in the region (Sanches et al., 2019; Schumacher et al., 2016; Teixeira and Prieto, 2020b), which highlight the intensification of the Low-Level Jet and moisture convergence in this season. Moreover, Sanches et al., (2019) reported a significant increase in extreme events in December and a reduction in return periods, which aligns with the elevated upward transition probabilities observed in our study (up to 0.2 in the Southern Shield).

In winter, by contrast, our analysis shows dominant downward transitions (e.g., Very Strong to Strong), suggesting that frontal systems prevailing during this season are more stable and less convective, consistent with the findings of Teixeira; Prieto, (2020a, 2020b). This mechanism favors less intense rainfall and reduces the likelihood of consecutive extreme events, in agreement with Britto; Barletta; Mendonça, (2006), who documented the frequent passage of cold fronts. Our results extend this evidence by showing that such systems quickly return to moderate conditions.

The persistence of Strong and Very Strong events in mountainous areas confirms that orography modulates the rainfall regime, enhancing air uplift and storm continuity during summer. In contrast, the rapid dissipation of extremes in the Central Depression and Coastal Plain reflects the flat topography, where the absence of orographic barriers limits convective

https://doi.org/10.5194/egusphere-2025-5114
Preprint. Discussion started: 15 January 2026

persistence. This is consistent with previous studies (Britto et al., 2006; Guedes et al., 2019; Teixeira and Prieto, 2020a) that identified persistent events associated with frontogenesis and slow-moving cyclogenesis in mountainous zones. Our results add detail by showing that these areas exhibit higher maximum intensities (9–11 mm h^{-1}) and greater persistence of Strong states, supporting the hypothesis that relief enhances both frontal and convective rainfall.

The higher upward transition probabilities observed in summer over the Southern Shield reflect mechanisms similar to those described for Mesoscale Convective Complexes (MCCs), where the Low-Level Jet (LLJ) and orography favor the persistence of intense rainfall. Ribeiro-Viana et al., (2009) reported 22 MCCs between October and December 2003, with an average duration of 18.6 hours, consistent with the persistence patterns identified in our study.

Storm characterization further revealed that rainfall events in lowland areas tend to last longer, which aligns with the increase in five-day precipitation totals (CMax5) documented by Minuzzi; Lopez, (2013). This suggests that storm persistence is a key driver of seasonal rainfall accumulation. The marked geomorphological contrasts in the study area also help explain why trend analyses do not show consistent signals across all stations, as highlighted by Melo; Louzada; Pedrollo, (2015). Orography not only influences trend detection but also affects the occurrence of extreme indices (R95p, R99p) (Melo et al., 2015) and the ICEXT index (Extreme Rainfall Intensity) analyzed by (Minuzzi and Lopez, 2013), both showing that relief can either attenuate or intensify extreme rainfall occurrence, producing spatially contrasting responses. Futhermore, across southern Brazil, including Paraná, Santa Catarina, and Rio Grande do Sul, multi-model projections from CMIP6 indicate stronger precipitation extremes through mid to late century. Intensity-based indices rise, with increases in RX1day and RX5day, very-wet and extremely-wet day totals (R95p, R99p), and the simple daily intensity index (SDII), alongside higher frequencies of heavy-rain days (R20mm) (Avila-Diaz et al., 2020).

The heterogeneous storm patterns driven by topography highlight the need for differentiated management strategies across physiographic units. The high persistence of rainfall in the Southern Shield indicates that this region may be an important source of runoff and sediment, suggesting the need for reforestation and soil management practices to reduce flood peaks. In the plains, where extreme events may lead to prolonged flooding, priority should be given to wetland restoration and the reinforcement of early warning systems to mitigate risks. (Marques and Möller, 2008), who studied water levels in the Lagoa dos Patos, emphasized that while storms dissipate in this ecosystem, water accumulation remains significant.

These management strategies are particularly relevant in light of evidence from previous studies pointing to an increasing trend in rainfall. (Guedes et al., 2019) reported that 50% of the stations they analyzed showed a significant increase in annual rainfall, linked to El Niño events. (Berlato et al., 2007) also demonstrated a generalized increase in precipitation in Rio Grande do Sul, associated with the higher frequency of El Niño. Such findings are concerning when considered alongside projections of increased El Niño frequency and intensity (Cai et al., 2014; Chen et al., 2024). Furthermore, Melo; Louzada; Pedrollo, (2015) estimated increases in R95p and R99p indices and projected up to 600 mm of additional annual rainfall above the 95th percentile by the end of the century in Rio Grande do Sul. Similarly, (Junges et al., 2019) found a significant increase of 6.3 mm/year in annual precipitation, with notable seasonal increases in spring (+2.5 mm/year) and winter (+1.9 mm/year).

https://doi.org/10.5194/egusphere-2025-5114
Preprint. Discussion started: 15 January 2026

5. Conclusions

The analysis revealed that summer is characterized by higher probabilities of transitions toward more intense storms, reaching values of up to 0.2, consistent with the intensification of the Low-Level Jet and the enhancement of orographic convection reported in previous synoptic studies. Conversely, winter is dominated by downward transitions, with probabilities approaching 0.95, reflecting the influence of more stable and homogeneous frontal systems.

Topography was found to play a decisive role in the persistence and dissipation of storms. In the Central Depression and the Coastal Plain, storms tend to last longer, with mean duration of 15 - 17 hours, but exhibit lower intensities, with average maximum values of 7 - 8 mm h^{-1}. In contrast, in the mountainous regions of the Southern Shield and the Southern Plateau, storms are more intense, with maximum intensities of 10 - 11 mm h^{-1}, but shorter-lived, lasting on average 11 – 12 hours. This pattern reflects the direct influence of relief on rainfall dynamics.

Overall, the spatial and temporal characterization of storms developed in this study provides a solid foundation for advancing early warning systems, guiding land-use planning adapted to distinct physiographic units, and supporting the design of adaptation strategies in response to the projected increase in extreme precipitation events in southern Brazil.

Appendix A1

Temporal homogeneity test results and chain order determination for seasonal Markov models

Season	Station	Order		Homogeneity	
		Chi^2	p-value	Chi^2	*p-value*
Spring	Bento Goncalves	3.383	0.496	3.457	0.485
	Cacapava do Sul	3.493	0.479	3.148	0.533
	Camaqua	4.078	0.396	4.29	0.368
	Canela	1.936	0.748	1.893	0.756
	Cangucu	2.973	0.562	2.991	0.559
	Cruz Alta	2.758	0.599	3.035	0.552
	Jaguarao	3.195	0.526	3.173	0.529
	Mostardas	2.471	0.65	2.563	0.634
	Passo Fundo	0.108	0.999	0.123	0.998
	Porto Alegre	2.599	0.627	2.587	0.629
	Rio Grande	2.511	0.643	2.489	0.647
	Rio Pardo	1.381	0.847	1.284	0.864
	São Gabriel	4.569	0.335	4.535	0.338
	Soledade	1.911	0.752	1.878	0.758
	Torres	1.94	0.747	0.425	0.98
Summer	Bento Goncalves	6.551	0.162	8.522	0.074
	Cacapava do Sul	1.558	0.816	1.832	0.767

https://doi.org/10.5194/egusphere-2025-5114
Preprint. Discussion started: 15 January 2026

	Camaqua	5.816	0.213	5.128	0.274
	Canela	0.898	0.925	0.994	0.911
	Cangucu	5.301	0.258	5.395	0.249
	Cruz Alta	0.418	0.981	0.666	0.955
	Jaguarao	4.99	0.288	3.531	0.473
	Mostardas	2.826	0.587	3.109	0.54
	Passo Fundo	2.367	0.669	2.304	0.68
	Porto Alegre	2.077	0.722	2.293	0.682
	Rio Grande	3.606	0.462	3.784	0.436
	Rio Pardo	3.851	0.427	3.683	0.451
	São Gabriel	1.851	0.763	1.889	0.756
	Soledade	2.506	0.644	2.714	0.607
	Torres	2.98	0.426	2.086	0.72
Fall	Bento Goncalves	3.623	0.459	3.587	0.465
	Cacapava do Sul	6.007	0.199	5.865	0.21
	Camaqua	6.169	0.187	6.136	0.189
	Canela	2.382	0.666	2.58	0.63
	Cangucu	2.379	0.666	2.368	0.669
	Cruz Alta	8.196	0.085	8.138	0.087
	Jaguarao	1.766	0.779	2.109	0.716
	Mostardas	4.502	0.342	4.458	0.348
	Passo Fundo	2.574	0.631	2.593	0.628
	Porto Alegre	1.204	0.878	1.671	0.796
	Rio Grande	10.067	0.056	9.896	0.056
	Rio Pardo	1.547	0.818	1.531	0.821
	São Gabriel	3.89	0.421	3.852	0.426
	Soledade	2.432	0.657	2.357	0.67
	Torres	0.425	0.98	1.346	0.854
Winter	Bento Goncalves	3.778	0.437	3.837	0.429
	Cacapava do Sul	4.736	0.315	6.89	0.142
	Camaqua	0.07	0.999	0.07	0.999
	Canela	0.153	0.997	0.152	0.997
	Cangucu	0.523	0.944	0.083	0.995
	Cruz Alta	0.647	0.958	0.647	0.958
	Jaguarao	0.171	0.997	0.171	0.997
	Mostardas	0.079	0.999	0.079	0.999
	Passo Fundo	1.167	0.883	1.184	0.881
	Porto Alegre	0.219	0.994	0.217	0.995

https://doi.org/10.5194/egusphere-2025-5114
Preprint. Discussion started: 15 January 2026

Rio Grande	9.564	0.052	9.605	0.052
Rio Pardo	1.486	0.829	1.486	0.829
São Gabriel	0.13	0.998	0.13	0.998
Soledade	0.284	0.991	0.284	0.991
Torres	1.3	0.861	0.079	0.98

Data availability

These data are publicly available from the Instituto Nacional de Meteorologia (INMET) at https://portal.inmet.gov.br/dadoshistoricos.

Author Contribution

Conceptualization: COM and JVS; data curation: COM and JVS; formal analysis: COM, JVS, JDMF, AAD, TAEF, DHM, and ASAS; Funding acquisition: COM; Methodology: COM, TAEF, DHM, and ASAS; Project administration: COM; Resources: COM; Software: COM and TAEF; Supervision: AAD and TAEF; Validation: TAEF, DHM and ASAS; Visualization: COM and JDMF; Writing (original draft preparation): COM, JVS, JDMF, and AAD; and Writing (review and editing): COM, JVS, JDMF, AAD, TAEF, DHM, ASAS.

Competing Interest

The authors declare that they have no conflict of interest.

Acknowledgements

The authors gratefully acknowledge the **Federal Rural University of Pernambuco (UFRPE)** and the **Graduate Program in Biometry and Applied Statistics (PPGBEA)** for their academic and scientific support throughout the development of this research. Special thanks are extended to the **Interdisciplinary Forecasting Research Oriented Group (IFROG)** for their valuable technical guidance and constructive discussions. The authors also express their appreciation to the **Instituto Nacional de Meteorologia (INMET)** for providing the meteorological data used in this study. Finally, The first and second author was supported by the Scholarship of the Coordenação de Aperfeiçoamento de Pessoal de Nível Superior—Brasil (CAPES) and The Conselho Nacional de Desenvolvimento Científico e Tecnológico (CNPq) of Brazil.

6. References

https://doi.org/10.5194/egusphere-2025-5114
Preprint. Discussion started: 15 January 2026

Agel, L., Barlow, M., Qian, J. H., Colby, F., Douglas, E., and Eichler, T.: Climatology of daily precipitation and extreme precipitation events in the Northeast United States, J Hydrometeorol, 16, 2537–2557, https://doi.org/10.1175/JHM-D-14-0147.1, 2015.

Alvalá, R. C. dos S., Ribeiro, D. F., Marengo, J. A., Seluchi, M. E., Gonçalves, D. A., Antunes da Silva, L., Cuartas Pineda, L. A., and Saito, S. M.: Analysis of the hydrological disaster occurred in the state of Rio Grande do Sul, Brazil in September 2023: Vulnerabilities and risk management capabilities, International Journal of Disaster Risk Reduction, 110, https://doi.org/10.1016/j.ijdrr.2024.104645, 2024.

Avila-Diaz, A., Benezoli, V., Justino, F., Torres, R., and Wilson, A.: Assessing current and future trends of climate extremes across Brazil based on reanalyses and earth system model projections, Clim Dyn, 55, 1403–1426, https://doi.org/10.1007/s00382-020-05333-z, 2020.

Back, Á. J. and Miguel, L. P.: Analysis of the stochastic model of the Markov chain on daily rainfall occurrence in the state of Santa Catarina, Brazil, Management of Environmental Quality: An International Journal, 28, 2–16, https://doi.org/10.1108/MEQ-07-2015-0135, 2017.

Berlato, M. A., Martins, E. J., Cordeiro, A. P. A., and Oderich, E. H.: Tendência observada da precipitação pluvial anual e estacional do estado do Rio Grande do Sul e relação com a temperatura da superfície do mar do Oceano Pacífico, Aracajú, https://doi.org/https://lume.ufrgs.br/handle/10183/34453, 2007.

Britto, F. P., Barletta, R., and Mendonça, M.: Regionalização sazonal e mensal da precipitação pluvial máxima no estado do Rio Grande do Sul, Revista Brasileira de Climatologia, 2, 35–51, https://doi.org/https://doi.org/10.5380/abclima.v2i0.25385, 2006.

Bühlmann, P. and Wyner, A. J.: Variable length Markov chains, The Annals of Statistics, 27, https://doi.org/10.1214/aos/1018031204, 1999.

Cai, W., Borlace, S., Lengaigne, M., Van Rensch, P., Collins, M., Vecchi, G., Timmermann, A., Santoso, A., Mcphaden, M. J., Wu, L., England, M. H., Wang, G., Guilyardi, E., and Jin, F. F.: Increasing frequency of extreme El Niño events due to greenhouse warming, Nat Clim Chang, 4, 111–116, https://doi.org/10.1038/nclimate2100, 2014.

Chen, Y., Zhao, C., and Zhi, H.: Analysis of ENSO Event Intensity Changes and Time–Frequency Characteristic Since 1875, Atmosphere (Basel), 15, https://doi.org/10.3390/atmos15121428, 2024.

Collischonn, W., Fan, F. M., Possantti, I., Dornelles, F., Paiva, R., Medeiros, M. S., Michel, G. P., Filho, F. J. C. M., Moraes, S. R., Marcuzzo, F. F. N., Michel, R. D. L., Beskow, T. L. C., Beskow, S., Fernandes, E. H. L., Dos Santos, L. L., Ruhoff, A., Kobiyama, M., Collares, G. L., Buffon, F., Duarte, E., Lima, S., Meirelles, F. S. C., and Piccilli, D. G. A.: The exceptional hydrological disaster of April-May 2024 in southern Brazil, Revista Brasileira de Recursos Hidricos, 30, https://doi.org/10.1590/2318-0331.302520240119, 2025.

Dorneles, V. R., Riquetti, N. B., and Nunes, A.: Forçantes dinâmicas e térmicas associadas a um caso de precipitação intensa sobre o Rio Grande do Sul, Brasil, Revista Brasileira de Climatologia, 16, https://doi.org/10.5380/abclima.v26i0.58162, 2020.

https://doi.org/10.5194/egusphere-2025-5114
Preprint. Discussion started: 15 January 2026

Gabriel, K. R. and Neumann, J.: A Markov chain model for daily rainfall occurrence at Tel Aviv, Quarterly Journal of the Royal Meteorological Society, 88, 90–95, https://doi.org/10.1002/qj.49708837511, 1962.

Gao, C., Guan, X., Booij, M. J., Meng, Y., and Xu, Y. P.: A new framework for a multi-site stochastic daily rainfall model: Coupling a univariate Markov chain model with a multi-site rainfall event model, J Hydrol (Amst), 598, https://doi.org/10.1016/j.jhydrol.2021.126478, 2021.

Guedes, H. A. S., Priebe, P. D. S., and Manke, E. B.: Tendências em séries temporais de precipitação no norte do estado do Rio Grande do Sul, Brasil, Revista Brasileira de Meteorologia, 34, 283–291, https://doi.org/10.1590/0102-77863340238, 2019.

Jale, J. da S., Xavier Júnior, S. F. A., Xavier, É. F. M., Stošić, T., Stošić, B., and Ferreira, T. A. E.: Application of Markov chain on daily rainfall data in Paraíba-Brazil from 1995-2015, Acta Scientiarum - Technology, 41, https://doi.org/10.4025/actascitechnol.v41i1.37186, 2019.

Jiang, Q., Cioffi, F., Conticello, F. R., Giannini, M., Telesca, V., and Wang, J.: A stacked ensemble learning and non-homogeneous hidden Markov model for daily precipitation downscaling and projection, Hydrol Process, 37, https://doi.org/10.1002/hyp.14992, 2023.

Junges, A. H., Bremm, C., and Fontana, D. C.: Rainfall climatology, variability, and trends in veranópolis, Rio Grande do Sul, Brazil, Revista Brasileira de Engenharia Agricola e Ambiental, 23, 160–166, https://doi.org/10.1590/1807-1929/agriambi.v23n3p160-166, 2019.

Kemsley, S. W., Osborn, T. J., Dorling, S. R., and Wallace, C.: Pattern scaling the parameters of a Markov-chain gamma-distribution daily precipitation generator, International Journal of Climatology, 44, 144–159, https://doi.org/10.1002/joc.8320, 2024.

Lamjiri, M. A., Dettinger, M. D., Ralph, F. M., and Guan, B.: Hourly storm characteristics along the U.S. West Coast: Role of atmospheric rivers in extreme precipitation, Geophys Res Lett, 44, 7020–7028, https://doi.org/10.1002/2017GL074193, 2017.

Marques, W. C. and Möller, O. O.: Variabilidade Temporal em Longo Período da Descarga Fluvial e Níveis de Água da Lagoa dos Patos, Rio Grande do Sul, Brasil, Revista Brasileira de Recursos Hídricos, 13, 155–163, https://doi.org/https://biblat.unam.mx/hevila/Revistabrasileiraderecursoshidricos/2008/vol13/no3/14.pdf, 2008.

Melo, T. M. de, Louzada, J. A. S., and Pedrollo, O. C.: Trends in Extreme indices and seasonal analysis of precipitation and temperature in the Northwest Region of Rio Grande do Sul, Brazili, Am J Clim Change, 04, 187–202, https://doi.org/10.4236/ajcc.2015.43015, 2015.

Minuzzi, R. B. and Lopez, F. Z.: Variabilidade de índices de chuva nos estados de Santa Catarina e Rio Grande do Sul, Original Article Biosci. J, 30, 697–706, https://doi.org/https://labclimagri.ufsc.br/files/bioscience_v30n3_2013.pdf, 2013.

Norris, J. R.: Markov Chains, Cambridge University Press, 1997.

Palecki, M. A., Angel, J. R., and Hollinger, S. E.: Storm Precipitation in the United States. Part I: Meteorological Characteristics, https://doi.org/https://doi.org/10.1175/JAM2243.1, 2005.

https://doi.org/10.5194/egusphere-2025-5114
Preprint. Discussion started: 15 January 2026

Ribeiro-Viana, D., Eliseu-Aquino, F., Burgobraga, R., and Ferreira, N. J.: Mesoscale convective complexes in Rio Grande do Sul between october and december of 2003 and associated precipitation, Revista Brasileira de Meteorologia, 24, 276–291, https://doi.org/https://doi.org/10.1590/S0102-77862009000300003, 2009.

Ross, S. M.: Introduction to Probability Models, Academic Press., 11th ed., 2014.

Sanches, F., Verdum, R., Fisch, G., Gass, S. L. B., and Rocha, V. M.: Extreme Rainfall Events in the Southwest of Rio Grande do Sul (Brazil) and Its Association with the Sandization Process, Am J Clim Change, 08, 441–453, https://doi.org/10.4236/ajcc.2019.84024, 2019.

Santos, E. B. and Barbosa Diniz, G.: Oceanic indices and their relations with the monthly precipitation in Rio Grande do Sul state, Brazil, Revista Brasileira de Geofísica, 32, 371–381, https://doi.org/ttp://dx.doi.org/10.22564/rbgf.v32i3.496, 2014.

Schumacher, V., Da, M., and Teixeira, S.: Relationship between instability indices and extreme rainfall in the state of Rio Grande do Sul, Brazil, Revista Brasileira de Geofísica, 34, 131–144, https://doi.org/http://dx.doi.org/10.22564/rbgf.v34i1.802, 2016.

Teixeira, M. da S. and Prieto, R. B.: Extreme rainfall events in the state of Rio Grande do Sul, Brazil, between 2004 and 2013. Part 1: Events definition and statistics, Revista Brasileira de Meteorologia, 35, 45–52, https://doi.org/10.1590/0102-7786351027, 2020a.

Teixeira, M. da S. and Prieto, R. B.: Extreme rainfall events in the state of Rio Grande do Sul, Brazil, between 2004 and 2013. Part 2: Synoptic characteristics of the persistent events, Revista Brasileira de Meteorologia, 35, 53–61, https://doi.org/10.1590/0102-7786351028, 2020b.

Valente, P. T., Viana, D. R., Aquino, F. E., and Simões, J. C.: Classification of precipitation anomalies in the Rio Grande do Sul in ENSO events in the 20th century, Sociedade & Natureza, 35, https://doi.org/10.14393/sn-v35-2023-66073, 2023.

Vargas, V. B., Corso, L., and Vallejos, R. V.: Markov chains to determine the probability of climate change for planting selection in the city of Caxias do Sul, Ciência Rural, 52, https://doi.org/10.1590/0103-8478cr20200840, 2022.

Wilks, D. S.: Statistical Methods in the Atmospheric Sciences, 3rd ed., Academic Press, 2011.